Concurrent Network Diakoptics for Electromagnetic Field Problems

L. N. Merugu and Vincent F. Fusco

Abstract—**This paper presents a new modification to circuit based diakoptics equations which allows the efficient manipulation of equivalent circuit models which represent Maxwell's equations. A new formulation of the diakoptics equations is given whereby torn subnetworks used to form the problem domain under consideration can be connected on a nearest neighbour basis. This formulation allows an algorithm to be written which is suitable for implementation on a parallel computer. In this work implementation is on a transputer array configured with two different topologies. The computational efficiency of each topology is appraised and considerable computational advantage demonstrated with respect to the classical sequential varient of the technique.**

The procedure is then applied to sample electromagnetic field problems in order to verify its utility. Finally it is used to compute the performance of a patch microstrip hybrid coupler.

I. Introduction

THE USE OF lumped electrical network equivalents to represent electromagnetic field quantities in the frequency domain is well-known [1]–[3]. However computation is notoriously slow or indeed impossible due to the large networks involved. This is true when conventional circuit analysis programs such as SPICE are used for solution. To overcome the computational difficulties encountered with large networks, concurrent diakoptics is developed here such that a large network can be solved piecewise [4].

The classical diakoptics method was developed by Kron [5], [6] to solve large physical problems by tearing the network into smaller pieces. In the past decade two major areas of application of diakoptics have emerged, one is field based, [7], [8] for the field analysis of antennas, and [9]–[11] for the field analysis of MMIC structures. The application of diakoptics (for EM field problems) using network models has received little attention [12], [13]. This paper considers a revision of the use of Kron's diakoptic method formulated by Brameller [14] to solve the network models of Maxwell's equations using novel concurrent programming techniques.

Simulation of electromagnetic behaviour of field problems at microwave and millimeter wave frequencies becomes computationally intensive for problems with complex geometry and generally requires high speed, large capacity computers. A parallel computer consisting of several processing units offers high speed and allows large problems to be solved by partitioning [15].

The motivation for the computational strategy adopted in this work is the availability of the INMOS transputer [16], a microprocessor exclusively designed to support concurrent parallel programming applications. The transputer has four bidirectional links used to communicate with other processors, thereby allowing various processor topologies to be constructed in order to form a general pupose low-cost parallel computer.

Application of parallel computing methods to electromagnetic problems is fairly recent [17]. Most reported applications have focused on the prediction of RF scattering, and calculations are normally pursued on expensive massively parallel computers [18]–[21]. As an alternative the transputer strategy used in this work to support a concurrent diakoptics algorithm offers a modular approach to the construction of a Multiple Instruction Multiple Date MIMD computer used as an adjunct to a personal computer [21]–[23]. Parallelism in the diakoptic methods comes from the property that the solution of one subnetwork does not depend on the solution of any other subnetwork, networks can therefore be solved simultaneously (concurrently).

In this work two different concurrent diakoptic equivalent circuit network algorithms are formulated and verified by modelling the field distribution of a rectangular waveguide, a microstrip line and a microstrip patch coupler. The results obtained show agreement with theory and validate the performance of the algorithms developed.

II. Electromagnetic Field Network Analogy

Maxwell's equations for an isotropic source free medium are

$$\nabla \times H = (\sigma + j\omega\epsilon)E$$
$$\nabla \times E = -j\omega\mu H \tag{1}$$

If the field is constant in one of the coordinates say y, so that $\partial/\partial y = 0$, the above set of field equations divide into two independent sets. The first set consists of Transverse Electric (TE) waves i.e., field components E_y, H_x and H_z. These can be expressed in finite-difference form as

$$E_y(x, z + \Delta z) - E_y(x, z) = j\omega\mu\Delta 1 H_x\left(x, z + \frac{\Delta z}{2}\right)$$
$$E_y(x + \Delta x, z) - E_y(x, z) = -j\omega\mu\Delta 1 H_z\left(x + \frac{\Delta z}{2}, z\right)$$

Manuscript received March 4, 1992, revised August 5, 1992.

The authors are with the Department of Electrical Engineering, The Queen's University of Belfast, Ashby Building, Stranmillis Road, Belfast BT9 5AH, N. Ireland.

IEEE Log Number 9206295.

$$H_x\left(x, z+\frac{\Delta z}{2}\right) - H_x\left(x, z-\frac{\Delta z}{2}\right) - H_z\left(x+\frac{\Delta x}{2}, z\right) + H_z\left(x-\frac{\Delta x}{2}, z\right) = (\sigma + j\omega\epsilon)\Delta 1 E_y(x,z) \quad (2)$$

where $\Delta 1 = \Delta x = \Delta z$. These equations can be used directly to solve field problems or can be abstracted into an electrical equivalent circuit form, [2], [27].

The finite-difference equations (2) can be represented by the RLC circuit shown in Fig. 1, Kirchhoff's loop equations are satisfied around meshes ABGA and ADGA, while Kirchhoff's current law is obeyed at the junction A. The voltage across the shunt capacitors correspond to E_y field and current through the series inductors correspond to H_x and H_z field [2]. Conducting boundaries can be applied by short circuiting the shunt capacitors. If a conducting boundary has a known nonzero conductivity or radiates this can be taken into account by terminating the network in an appropriate impedance [28]. In the work presented here radiation effects are not included, and unless otherwise stated all boundaries are assumed ideal. Boundary excitation is applied by connecting voltage or current generators to the boundary nodes of the network, the amplitude and/or phase of these is defined by the particular problem under investigation.

The model cell given in Fig. 1 is duplicated inorder to fill the space occupied by the real problem, thereby forming a highly regular grid of network elements. Thus implying implementation of the network solution using parallel computing techniques based on concurrent diakoptics algorithms.

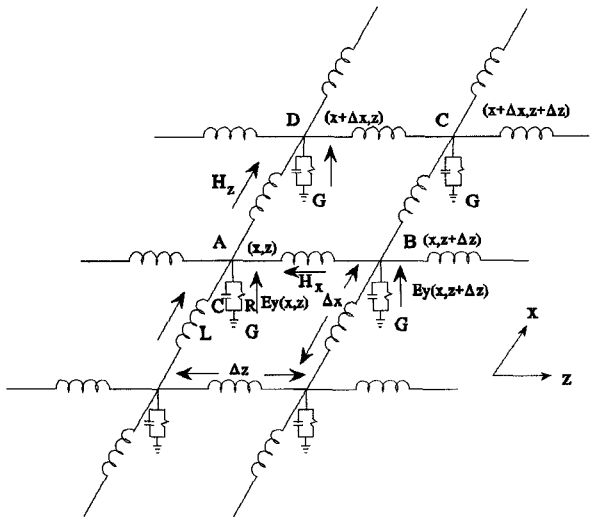

Fig. 1. 2-D Network analog for TE waves in Cartesian coordinates.

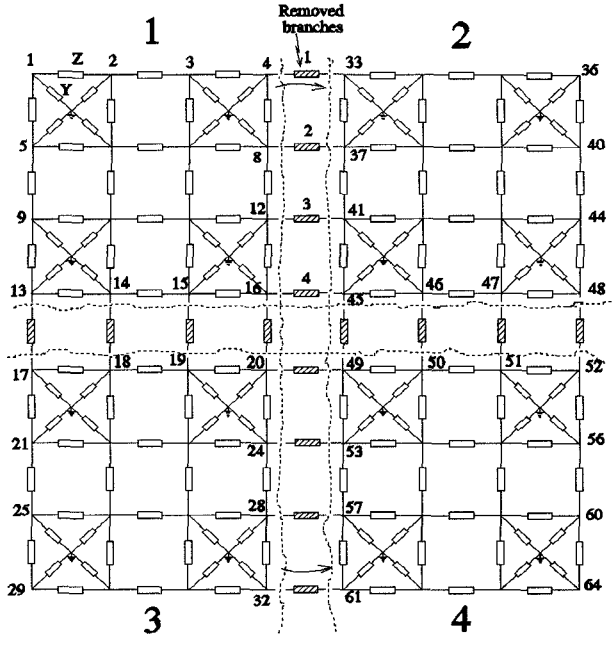

Fig. 2. Illustration of 64 node network torn into 4 Subnetworks.

III. Circuit Based Diakoptics

In order to solve a large system in a piecewise manner the system itself, or an abstract version of it, its branch network model, is dissected into n parts. After solving each part separately, the n pieces are reconnected to form the solution of the original problem. As a result the final reassembled piecewise solution is the same as that for the same network analyzed, in totality.

There are several advantages to piecewise solution of a physical system in comparison to the conventional method of solving an entire problem as one unit.

1. Large problems that could not be solved before due to limited computing capacity can now be solved by the diakoptics method.

2. The accuracy of the solution depends on the size of the subdivisions and not on the size of the original network.

3. Considerable savings in computation time can be achieved. For instance inversion of a matrix by diakoptics results in a CPU reduction of $2/n^2$, where n is the number of subdivisions.

4. If two or more subnetworks are the same, then only one subnetwork need be solved.

5. If a system is modified then only the subnetworks of the modified portion need to be solved again since the rest of the solution remains unchanged, so that solutions evolve with the physical system.

6. A library of subsolutions can be maintained so that they can be interconnected as and when required.

7. Each subnetwork can be manipulated independently of every other. This allows scope for efficient parallelization of the solution which has ramifications for the solution in terms of 1–6 above.

The fundamental equations of diakoptics using nodal analysis terminology are discussed fully in [14] where a general exposition including sources in the removed branches (useful for solid state modelling) is given. The method proceeds by tearing the composite network in Fig. 2 into a number of subnetworks (equivalent networks) each with an admittance matrix $\tilde{Y}_{jj}$.

The admittance matrix $[\tilde{Y}]$ of the composite network has a

block diagonal form,

$$\tilde{Y}_{\alpha\alpha} = \begin{bmatrix} \tilde{Y}_{11} & 0 & \cdots & \cdots & 0 \\ 0 & \tilde{Y}_{22} & 0 & \cdots & 0 \\ \cdots & \cdots & \cdots & \cdots & \cdots \\ 0 & 0 & 0 & \cdots & \tilde{Y}_{nn} \end{bmatrix}. \quad (3)$$

The block diagonal form of (3) is an essential element of this method since inversion of the matrix is obtained by inverting each of the individual submatrices along the diagonal.

The resulting diakoptic equations can be written as

$$V_\alpha = \tilde{Y}_{\alpha\alpha}^{-1} I_\alpha - \tilde{Y}_{\alpha\alpha}^{-1} C_{\alpha\psi} \tilde{Z}_{\psi\psi}^{-1} C_\alpha^t \tilde{Y}_{\alpha\alpha}^{-1} I_\alpha \quad (4)$$

where

$$\tilde{Z}_{\psi\psi} = Z_{\psi\psi} + C_{\psi\alpha}^t \tilde{Y}_{\alpha\alpha}^{-1} C_{\alpha\psi}$$

which is used to solve for the network unknown nodal voltages, V_α with I_α as the excitation current vector. In (4) $Z_{\psi\psi}$ is the removed element matrix, and $C_{\psi\alpha}$ is the connection matrix used to interconnect the subnetworks. These definitions and their derivations are fully discussed in [14] to which the reader can refer for more detail. Equation (4) and special concurrent derivatives of it are used as the basis for the work described in this paper. Concurrent algorithms will be developed to solve the equations represented by (4). Due to its block diagonal form (4) takes full advantage of network tearing by inverting the equivalent admittance matrix $[\tilde{Y}]$ piecewise.

IV. Parallel Algorithm Design

Many physical problems have a geometrical structure with spatially limited interaction between non-adjacent discretized cells. The problem geometry can therefore be divided into a number of parts and each part can be assigned to a different processor, the processors communicating with their nearest neighbors. It is always preferable to implement the hardware configuration in such a way that the processor array has the same geometry as that of the system being simulated [29]. This is the basic technique adopted in this work and is supplemented by algorithmic parallelism. Algorithmic parallelism is achieved by identifying parts of the algorithm supporting concurrent operation, each part may then be executed on a different processor to obtain speed-up. For convenience all of the algorithms used in this work are programmed in 3L PARALLEL FORTRAN [30] which is a concurrent varient of ANSI FORTRAN 77.

V. Diakoptic Algorithm for Network Solutions

In this section diakoptic algorithms are developed to construct a fast electromagnetic field computing technique. The network based diakoptic algorithms developed here are used to model the two-dimensional field network analogs described previously.

Fig. 2 represents a medium that can be used to model Maxwell's equations in 2-dimensional space. The size of such a network for a given application depends on the field resolution required and in general this results in a large network, solution of which by direct network solution methods may be very inefficient thus often computationally infeasible. The method presented in this work is essentially a two dimensional lumped circuit representation of the classical finite difference form of Maxwell's equations. This method of representation has several advantages when compared with finite difference or finite element electromagnetic field formulations. The primary advantage is that the repetitive networks describing the electromagnetic field connect on a nearest neighbor basis, this implies natural concurrency therefore the potential for highly efficient parallel algorithms. Natural concurrency is difficult to find in finite difference of finite element formulations other than at the equation assembly phase, although special concurrent matrix solvers [35] could be brought to bear latter in the solution cycle. The accuracy of the network modelling approach is restricted only by the normal requirements of lumped element descriptions of distributed circuits and does not suffer from numerical convergence difficulties associated with other methods. In addition the network modelling method is very suited for direct integration with active device lumped equivalent circuit models, this is not generally the case with alternate field based approaches. This aspect of the modelling strategy adopted in this work is currently this subject of a separate study.

TABLE I
Computation Time for Different Size Using Sequential Algorithm

Size of Network (Nodes)	Computation Time (Seconds)		Time Ratio
	1 X T800 (T1)	PC386/387 (T2)	T2/T1
88	4.67	11.53	2.47
132	6.82	19.95	2.92
176	10.93	36.10	3.30
264	27.07	101.48	3.75
352	58.00	227.75	3.93
440	108.42	435.00	4.01
528	183.34	743.24	4.05
616	287.31	1172.47	4.08
704	425.50	1741.76	4.09

The diakoptics method implemented in the following sections allows the solution of large systems in a computationally feasible way. The results in Table I are for classical implementation of the diakoptics algorithm. This computes subnetworks serially and interconnects the subsolutions on a global basis to form the solution for the original problem, (4).

Matrix products $C_{\alpha\psi} V_\psi$, $C_{\psi\alpha}^t V_\alpha$ and $C_{\psi\alpha}^t \tilde{Y}_{\alpha\alpha}^{-1} C_{\alpha\psi}$ in (4) can be reduced to algebraic summations which contribute significant savings in computation time irrespective of whether the algorithm is serial or parallel. This is achieved by storing the connection matrix in condensed form [14]. Throughout this work the connection matrix is used in its condensed form, this results in computer time savings of about 40% for typical problems [4].

Computation times obtained on a single transputer and those for a PC with coprocessor for the sequential algorithm for network sizes ranging from 88 nodes to 704 nodes is given in Table I, in each case the network is subdivided into four subnetworks.

VI. Concurrent Diakoptic Algorithms

Further improvements in the performance of the diakoptics algorithms are now investigated by applying parallel computing techniques. The interconnection of subnetworks on a global basis requires the matrix $\tilde{Z}_{\psi\psi}$ in (4) which in turn depends on the solutions of all subnetworks. If the subnetwork solutions are communicated to a master process, the communication time may outweigh the advantage obtained by solving the subnetworks in parallel. Since the interconnection of subnetworks cannot start until all the solutions of the subnetworks are available, the processors solving the subnetworks become idle as soon as they transfer the solution to the master, thereby leading to inefficient utilization. This problem can be circumvented by introducing a nearest neighbor interconnection methodology.

A. Nearest Neighbor Subnetwork Interconnection

The nearest neighbor reformulation of (4) for a simple two subnetwork arrangement is given by (5), (6).

$$\begin{bmatrix} V_1 \\ V_2 \end{bmatrix} = \begin{bmatrix} \tilde{Y}_1^{-1} & 0 \\ 0 & \tilde{Y}_2^{-1} \end{bmatrix} \begin{bmatrix} I_1 \\ 0 \end{bmatrix} - \begin{bmatrix} \tilde{Y}_1^{-1} & 0 \\ 0 & \tilde{Y}_2^{-1} \end{bmatrix} \cdot \begin{bmatrix} C_1 \\ C_2 \end{bmatrix} \tilde{Z}^{-1} [C_1^t \quad C_2^t] \begin{bmatrix} \tilde{Y}_1^{-1} & 0 \\ 0 & \tilde{Y}_2^{-1} \end{bmatrix} \begin{bmatrix} I_1 \\ 0 \end{bmatrix} \quad (5)$$

where

$$\tilde{Z} = Z + C_1^t \tilde{Y}_1^{-1} C_1 + C_2^t \tilde{Y}_2^{-1} C_2 \quad (6)$$

here, 1, 2 refer to the independent subnetworks 1 and 2 and $\tilde{Z}$ refers to the matrix formed via connection branch elements. $C_{1,2}$ are the connection matrices describing the interconnection of branch elements to subnetworks 1 and 2 respectively. The process of forming larger subnetworks from smaller subnetworks will be called folding.

B. Network Folding Algorithms

In general diakoptics formulation, the connection of one pair of subnetworks does not depend on that of any other pair. thus a number of interconnection processes can be implemented in parallel. For instance the subnetworks (1, 2) and (3, 4) shown in Fig. 3 can be connected simultaneously on the nearest neighbor basis. The operation of this algorithm is similar to paper folding with each incremental circuit element forming a hinged square, thus the term ORIGAMI algorithm is proposed [24]–[26].

In the ORIGAMI algorithm each of the processes numbered 1 to 4 in Fig. 3 computes concurrently the nodal admittance matrix of a piece of the network. Interconnection of the subnetworks can then be carried out concurrently on the nearest neighbor basis. For example in Fig. 3, the network can be folded in two stages, in the first stage subnetworks SN1 and SN2 can be folded to form a larger subnetwork denoted by SN(1, 2). The order of this resultant subnetwork is the sum of the orders of the subnetworks SN1 and SN2. Simultaneously, folding of another pair of subnetworks SN3 and SN4 can be performed to form another larger subnetwork SN(3, 4).

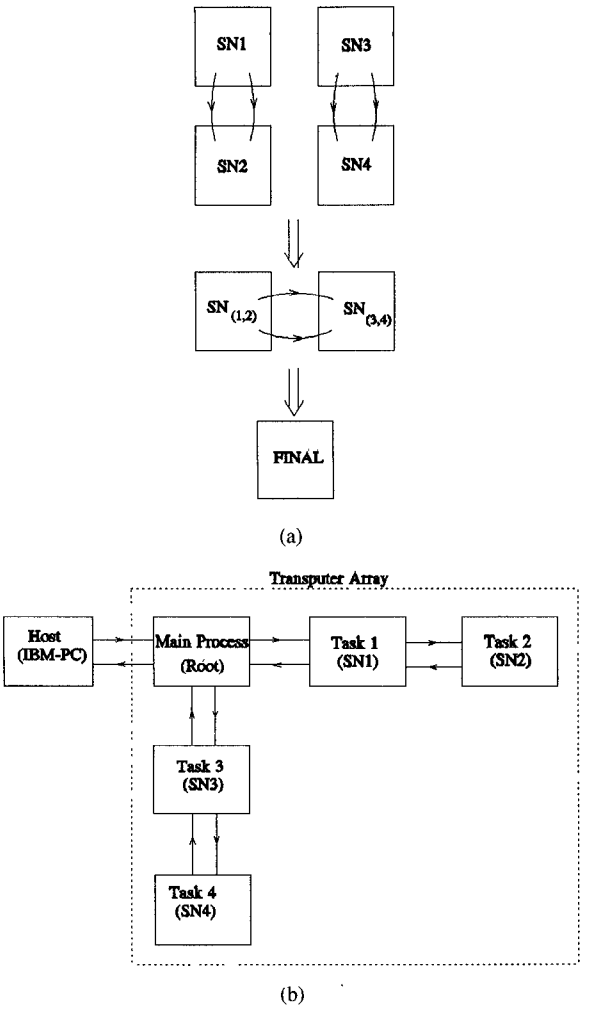

Fig. 3. Network folding ORIGAMI algorithm and task distribution.

In the second stage the compound subnetworks SN(1, 2) and SN(3, 4) can be joined to form the solution of the network using (5) and (6). In general for a network divided into 2^m subnetworks the nearest neighbor joining method requires m stages of folding in order to arrive at the final solution. The next $(m-1)$ stages fold the smaller subnetworks to form larger subnetworks by the following equations

$$\tilde{Y} = \begin{bmatrix} \tilde{Y}_n^{-1} & 0 \\ 0 & \tilde{Y}_{n+1}^{-1} \end{bmatrix} \begin{bmatrix} C_n \\ C_{n+1} \end{bmatrix} \tilde{Z}^{-1} \cdot [C_n^t \quad C_{n+1}^t] \begin{bmatrix} \tilde{Y}_n^{-1} & 0 \\ 0 & \tilde{Y}_{n+1}^{-1} \end{bmatrix} \quad (7)$$

where

$$\tilde{Z} = Z + C_n^t \tilde{Y}_n C_n + C_{n+1}^t \tilde{Y}_{n+1}^{-1} C_{n+1}$$

n and $n+1$ in the above equations refer to the adjacent subnetworks n and $n+1$. C_n and C_{n+1} are the partitioned connection matrices local to the subnetworks. The computation times obtained for the algorithm of Fig. 3 are given in Table II.

From Table II the improvement in speed-up on a 4 transputer network is not significant when compared to that on a 2 transputer network. The reason is due to the local interconnection process explained in Fig. 3(a). Here when one processor communicates its solution to the adjacent processor it will be

TABLE II
COMPUTATION TIMES ON NETWORK FOLDING ORIGAMI ALGORITHM

Size of Network (Nodes)	Computation Time (Seconds)			Speed-up	
	1 X T800 (T1)	2 xT800 (T2)	4 X T800 (T3)	T1/T2	T1/T3
88	3.46	1.81	1.53	1.91	2.26
132	8.41	4.28	3.46	1.96	2.43
176	16.75	8.52	6.60	1.96	2.53
264	47.24	23.95	17.58	1.97	2.68
352	102.00	51.60	36.80	1.97	2.77
440	188.34	94.97	66.35	1.98	2.83
528	312.91	-	107.93	-	2.90

idle for the rest of the problem. For instance in the algorithm of Fig. 3(b) the transputer executing task 2, computes the subnetwork solution and communicates it to the processor executing task 1 and will be idle for the rest of the problem. If the algorithm is executed on 4 processors, after the first stage of interconnection 2 processors executing task 2 and task 4 will be idle. The main process is placed on the root processor executing task 1.

In general if the algorithm has 2^m tasks and each task solves a subnetwork on an independent processor, then half the number of processors will become inactive after connecting of each stage until $(m-1)$ stages of interconnections. The processor utilization may be improved by placing more than one task on a processor. However the accumulation of subnetworks leads to memory storage limitations on individual processors. As a result of this the ORIGAMI algorithm is effective only for small to medium sized problems, c.f. Table I.

The limitations of the ORIGAMI algorithm explained above may be overcome by updating the subnetwork solutions locally. The RING algorithm is designed for problems which can be partitioned such that each subnetwork communicates with its successor and predecessor, hence the subnetworks form a chain (or a ring) of processes shown in Fig. 4(a). Large problems can be handled by folding the processes locally (Fig. 4(b)). Hence a network representing a field problem with complex geometry can be efficiently modelled by partitioning the geometry into four major subnetworks which communicate with each other in a pipe or ring structure, Fig. 4(c).

The Appendix describes a mathematical formulation to fold a four subnetwork problem which can be mapped onto a ring of transputers. In the ring algorithm a subnetwork does not send its full solution say, (mxm matrix to its neighbor, instead it now sends only a (ψxψ) matrix in which ψ is the number of removed branches local to the two adjacent subnetworks. Since there is no subnetwork accumulation as there is in the ORIGAMI algorithm, much larger problems can be efficiently solved.

The RING algorithm shown in Fig. 4(a) was mapped onto a two and a four transputer network. The computation times for three sizes of networks obtained on a 1, 2 and 4xT800 transputers are given in Table III. It can be seen from Table III that the RING algorithm is more efficient than the ORIGAMI algorithm.

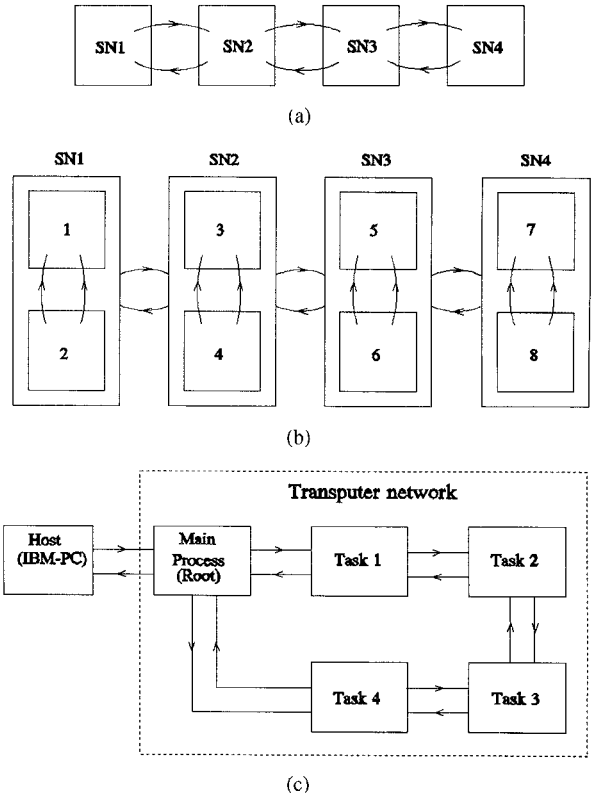

Fig. 4. Network folding RING algorithm and task distribution. (a) Simple process partitioning. (b) Composite process partitioning. (c) Mapping of processes onto a ring of transputers.

TABLE III
COMPUTATION TIMES ON NETWORK FOLDING RING ALGORITHM

Size of Network (Nodes)	Computation Time (Seconds)			Speed-up	
	1 X T800 (T1)	2 xT800 (T2)	4 X T800 (T3)	T1/T2	T1/T3
88	4.07	3.35	2.52	1.21	1.61
132	5.00	2.81	1.82	1.78	2.75
176	10.77	5.66	3.62	1.90	2.97
264	34.00	17.47	10.98	1.94	3.09
352	78.76	40.15	25.10	1.96	3.14
440	151.92	77.28	48.11	1.96	3.16
528	260.73	132.32	82.33	1.97	3.16
616	412.10	208.83	129.90	1.97	3.17
704	606.00	304.62	190.81	1.99	3.17

VII. PERFORMANCE OF THE DIAKOPTIC ALGORITHM

The computational performance of the network folding algorithms are compared by contrasting Tables I, II, III. Computation is enhanced by about 3.17 times over that on a single transputer i.e., 2.2 times over the sequential algorithm. The ORIGAMI algorithm could not be used to solve the 704 node network because of memory limitations associated with the transputer. When the size of the network is doubled from 352 nodes to 704 nodes, the computation time increased by a factor of 7 to 8 times for all cases, primarily due to the solution of subnetwork elements.

TABLE IV
COMPUTATION TIMES ON NETWORK FOLDING RING ALGORITHM USING ORIGAMI METHOD FOR SUBNETWORK FOLDING

NWS (Nodes)	MSN	SSN in MSN	Computation Time (Sec.)			Speed-up	
			1XT800 (T1)	2xT800 (T2)	4XT800 (T3)	T1/T2	T1/T3
352	4	2	31.80	16.31	10.31	1.95	3.08
		4	22.73	11.70	7.42	1.94	3.06
528	4	2	90.35	45.92	28.72	1.97	3.14
		3	65.64	33.34	20.93	1.97	3.14
		4	54.65	27.79	17.46	1.97	3.13
704	4	2	196.25	99.19	61.91	1.98	3.17
		4	105.13	53.17	33.34	1.98	3.15

NWS - Network Size
MSN - Major Subnetworks
SSN - Smaller Subnetworks

In the network tearing approach there is no fixed limit to the size of the subnetwork, and to the number of pieces; however, it is usual to define a primitive element as that having the smallest size that can be conveniently replicated. The size of a subnetwork influences overall computation time for the solution of a large network. A considerable computational advantage using the RING algorithm is obtained by dividing each subnetwork of a large network further into small subnetworks as shown in Table IV. This time the 704 node problem reduces to 196.25 and 105.13 seconds, Table IV when each subnetwork is further split into 2 and 4 small subnetworks. It should be noted that speed-up for the networks sizes given in Table IV is nearly the same as that given in Table III, but the overall computation time is considerably reduced, an overall speed-up of 10 to 18 times is obtained. As discussed above the RING algorithm is most effective when large networks are considered. This can be seen in Table III where minimum processor times occur for the 132 node problem. For smaller network sizes processor latency reduces computational advantage.

VIII. VERIFICATION OF THE NETWORK DIAKOPTICS METHOD

The concurrent diakoptics method is now applied to a waveguide problem. To satisfy the required boundary conditions the side walls of the waveguide are connected to ground, input excitation is applied by connecting current generators to the boundary nodes. A signal of unit amplitude with constant phase is applied across the waveguide aperture. The classical waveguide structure adopted here is chosen because of its analytical solubility hence its appeal as a benchmark check for accuracy of solution. A standard WR-90 rectangular waveguide of length one wavelength long at 10 GHz can be represented by a network of $(14\delta l \times 24\delta l)$: this represents a mesh discretization of $\lambda/20$.

The network describing the waveguide problem is divided into four pieces and solved on a T800 transputer network using concurrent network folding algorithms. Fig. 5 presents the E_y field (proportional to V_y) distribution in the z-direction for two different mesh sizes obtained on application of the folding

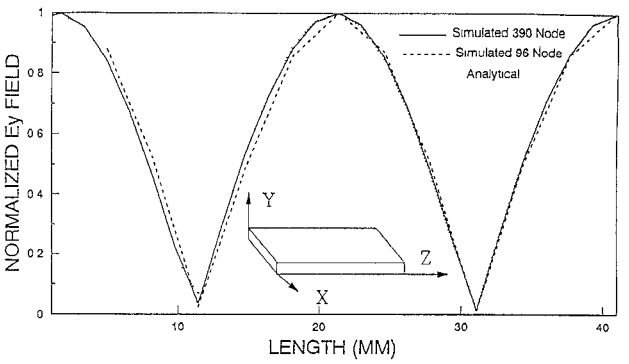

Fig. 5. $|E_y|$ Field in an ideal open ended rectangular waveguide, along the Z direction.

algorithms. Comparison of the results obtained by simulation with the analytical results shows that a mesh size of 20 units per wavelength is sufficient to describe the fields in a straight waveguide section.

Often fine detail of field behavior within the transmission line or structure under investigation is not required. In these cases the scattering parameter matrix can be obtained directly from port voltage and current relationships.

IX. APPLICATION OF NETWORK ANALOGS TO PLANAR CIRCUITS

Since the concurrent diakoptics method network as described here allows the modelling of a general two-dimensional medium, it can be applied to problems such as microstrip using equivalent waveguide modelling and planar circuit techniques, [31]–[33].

The frequency dependent properties of the microstrip line can now be described by using the appropriate values of L and C on the lumped equivalent network:

$$L = \mu_0 \Delta l$$
$$C = \epsilon_0 \epsilon_{r,\text{eff}}(f) \Delta l \tag{8}$$

The frequency dependent effective permittivity $\epsilon_{r,\text{eff}}(f)$ can be computed from a standard microstrip dispersion model. The frequency dependent effective width, $W_{\text{eff}}(f)$ of the parallel plate waveguide is calculated after Kompa [33] for a 50 ohm microstrip line on a 0.79 mm Duroid substrate with relative permittivity of 2.2 at 13.0 GHz, the cut-off frequency for the model is 41.4 GHz.

The width of the line is divided into 10 mesh units, this corresponds to a mesh size smaller than $\lambda_g/40$ at 13.0 GHz. The length of the microstrip modelled is about 1.47 λ_g long, and is divided into 63 mesh units. Current sources of unit amplitude and constant phase are connected at the input boundary nodes and the RING algorithm is used for solution. On the network an impedance of 270 ohms connected at each of the input and output boundary nodes giving a VSWR of 1.07. This impedance corresponds to the wave impedance Z_w of the parallel plate waveguide filled with dielectric. The microstrip line characteristic impedance, Z_0, can be computed

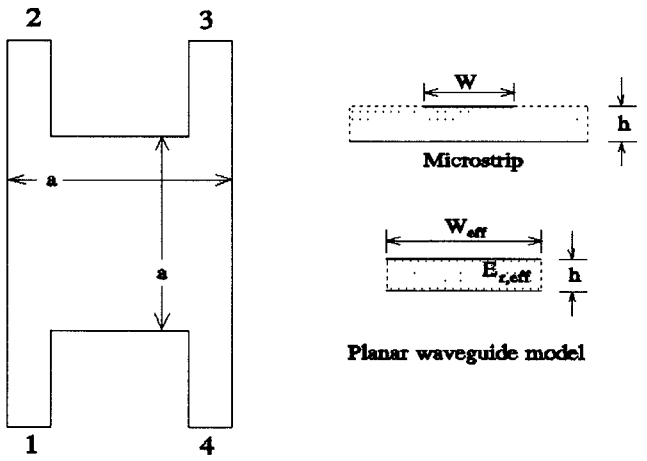

Fig. 6. Square microstrip patch coupler. $f = 13.0$ GHz; $E_r = 2.2$. $h = 0.79$ mm; $a = 8.66$ mm.

from the wave impedance as

$$Z_0 = \left(\frac{b}{a}\right) Z_w \tag{9}$$

where a is width and b is height of parallel plate waveguide. This results in a characteristic impedance of 49.5 ohms. When the output port is terminated in a short circuit, the distance between the two successive minima of the VSWR pattern was one half the guide wavelength. A VSWR of 2.0 and 4.0 for the output terminations corresponding to $Z_0/2$ and $Z_0/4$, these values are commensurate with standard theory. The computed magnitude of S_{11} and S_{21} when compared with the results obtained by classical theory show agreement.

X. Simulation of Patch Coupler

The dynamic planar waveguide concept explained previously is now applied to model the microstrip patch coupler shown in Fig. 6. This work approximates the microstrip patch coupler [34] by an equivalent planar waveguide model which is then represented by the lumped equivalent network and solved by the diakoptic method.

The square microstrip patch coupler shown in Fig. 6 is sub-divided into five parts, parts 1 to 4 represent the feed arms and the fifth part represents the square resonator. Once each individual microstrip section is replaced by the equivalent planar waveguide, their interconnection forms the equivalent waveguide configuration for the square patch microstrip coupler. The physical dimension, a, of the square patch was 8.66 mm at 13 GHz, arrived at empirically by TLM simulation [34]. In the computation, a, was replaced by the frequency dependent effective width $W_{p,\text{eff}}(f)$ of the patch, calculated to be 11.10 mm. The microstrip feed width of 2.44 mm when replaced by planar waveguide gives a width of 3.889 mm.

The values of L and C of the network model are computed from equation (8). Loss and radiation effects can be introduced by calculating approximate resistive components form [28]. It should be noted that the two different line widths associated with this structure viz. the feed arm and the patch have different $\epsilon_{r,\text{eff}}$, hence two different sets of values of L, C. A uniform mesh size of 0.74 mm is selected to represent the

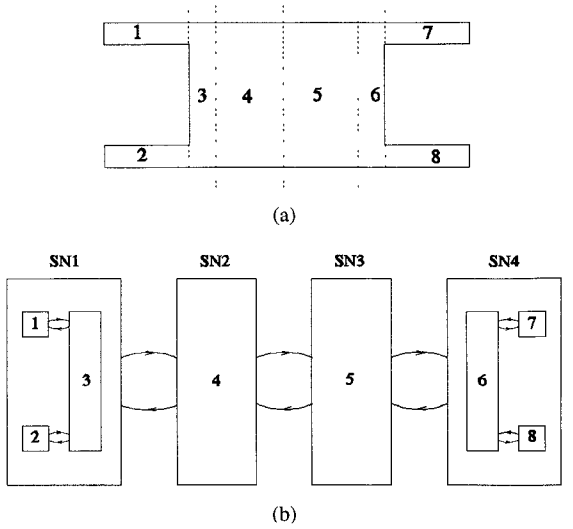

Fig. 7. Network folding RING algorithm used to map patch coupler onto a transputer array. (a) Schematic representation of network of patch coupler divided into small subnetworks. (b) Subnetwork folding for RING algorithm.

TABLE V
Computed S-Parameters of a Square Microstrip Patch Coupler at 13.0 GHz

S-parameters	$\epsilon_{r,\text{eff}}$ (Uniform)	$\epsilon_{r,\text{eff}}$ (Structure dependent)
$\lvert S_{11}\rvert$	0.1273 (-17.90 dB)	0.1561 (-16.13 dB)
$\lvert S_{21}\rvert$	0.7040 (-3.05 dB)	0.6985 (-3.12 dB)
$\lvert S_{31}\rvert$	0.6781 (-3.37 dB)	0.6746 (-3.42 dB)
$\lvert S_{41}\rvert$	0.2228 (-13.04 dB)	0.2277 (-12.85 dB)
$\angle S_{31} - \angle S_{21}$	-91.54°	-92.54°

coupler geometry, this corresponds to $\lambda_g/22$ at 13 GHz. The network is divided into eight subnetworks shown in Fig. 7.

The subnetworks that are folded locally to form four major subnetworks which is the requirement for the RING algorithm as shown in Fig. 7(b). The S-parameters of the patch coupler computed from the network nodal voltages across the feedline apertures are given in Table V, these results justify hybrid quadrature behavior.

XI. Conclusion

A new algorithm is developed which is suitable for interconnecting on a nearest neighbor basis the massively repetitive equivalent circuits that result when network analogs are used to represent electromagnetic field quantities. The algorithm is efficient for operation on a parallel computer. The effect of parallel process interconnection on comptational efficiency has been demonstrated. Further it has been shown that two dimensional equivalent circuit networks allow modelling of planar microwave structures. This suggests that when the network diakoptics method is combined with planar waveguide concepts it can be used as an alternative approach to the

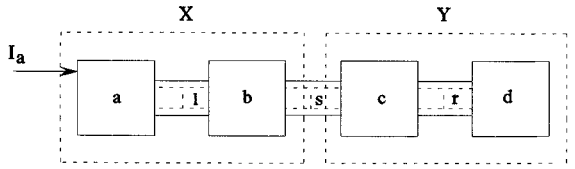

Fig. 8. Nearest neighbor network reduction for a four subnetwork problem: excitation vector I_a.

segmentation method [28]. This is particularly so if field detail within elements is required. The method has been verified on sample transmission line problems and has been used to model the behavior of a recently introduced microwave component the Patch Hybrid Coupler.

APPENDIX

NETWORK REDUCTION METHOD FOR FOUR SUBNETWORKS

The basic global diakoptics (4) can not easily be extended to update the subnetwork solutions locally for more than two subnetworks. Principally this is due to partitioning of the matrix (4) formed by the removed branches $\tilde{Z}_{\psi\psi}$, on a subnework basis becomes difficult. This Appendix describes the mathematical formulation to fold the four subnetwork situation illustrated in Fig. 8.

In Fig. 8 each subnetwork communicates with its predecessor and its successor. Nodal voltages V, on the network are computed for the excitation I applied to the subnetwork a. The network of Fig. 8 can be treated as having two major subnetworks X and Y for which the nodal voltages can be written using (4):

$$V_X = \tilde{Y}_{XX}^{-1} I_X - \tilde{Y}_{XX}^{-1} C_{Xs} \tilde{Z}_{ss}^{-1} C_{sX}^t \tilde{Y}_{XX}^{-1} I_X \quad \text{(A1.1)}$$

$$V_Y = -\tilde{Y}_{YY}^{-1} C_{Ys} \tilde{Z}_{ss}^{-1} C_{sX}^t \tilde{Y}_{XX}^{-1} I_X \quad \text{(A1.2)}$$

where

$$\tilde{Z}_{ss} = Z_{ss} + C_{sX}^t \tilde{Y}_{XX}^{-1} C_{Xs} + C_{sY}^t \tilde{Y}_{YY}^{-1} C_{Ys}, \quad \text{(A1.3)}$$

Z_{ss} is formed by s removed branches and the connection matrices C_{sX} and CsY are local to the torn subnetworks X and Y.

Since the subnetwork X consists of two smaller subnetworks a and b the equivalent nodal admittance matrix $\tilde{Y}_{XX}$, can be written as

$$\tilde{Y}_{XX}^{-1} = \begin{bmatrix} Z'_{aa} & Z'_{ab} \\ Z'_{ba} & Z'_{bb} \end{bmatrix} \quad \text{(A1.4)}$$

where

$$\begin{aligned} Z'_{aa} &= \tilde{Y}_{aa}^{-1} - \tilde{Y}_{aa}^{-1} C_{al} \tilde{Z}_{ll}^{-1} C_{la}^t \tilde{Y}_{aa}^{-1} \\ Z'_{ab} &= -\tilde{Y}_{aa}^{-1} C_{al} \tilde{Z}_{ll}^{-1} C_{lb}^t \tilde{Z}_{bb}^{-1} \\ Z'_{ba} &= -\tilde{Y}_{bb}^{-1} C_{bl} \tilde{Z}_{ll}^{-1} C_{la}^t \tilde{Y}_{aa}^{-1} \\ Z'_{bb} &= \tilde{Y}_{bb}^{-1} - \tilde{Y}_{bb}^{-1} C_{bl} \tilde{Z}_{ll}^{-1} C_{lb}^t \tilde{Y}_{bb}^{-1} \end{aligned} \quad \text{(A1.5)}$$

and

$$\tilde{Z}_{ll} = Z_{ll} + C_{la}^t \tilde{Y}_{aa}^{-1} C_{al} + C_{lb}^t \tilde{Y}_{bb}^{-1} C_{bl}, \quad \text{(A1.6)}$$

Z_{ll} is the Z matrix formed by l removed brances, and C_{al} and C_{bl} are connection matrices local to the subnetworks a and b.

Similarly the nodal admittance matrix $\tilde{Y}_{YY}$ for the subnetwork Y can be written as

$$\tilde{Y}_{YY}^{-1} = \begin{bmatrix} Z'_{cc} & Z'_{cd} \\ Z'_{dc} & Z'_{dd} \end{bmatrix} \quad \text{(A1.7)}$$

where

$$\begin{aligned} Z'_{cc} &= \tilde{Y}_{cc}^{-1} - \tilde{Y}_{cc}^{-1} C_{cr} \tilde{Z}_{rr}^{-1} C_{rc}^t \tilde{Y}_{cc}^{-1} \\ Z'_{cd} &= -\tilde{Y}_{cc}^{-1} C_{cr} \tilde{Z}_{rr}^{-1} C_{rd}^t \tilde{Z}_{dd}^{-1} \\ Z'_{dc} &= -\tilde{Y}_{dd}^{-1} C_{dr} \tilde{Z}_{rr}^{-1} C_{rc}^t \tilde{Y}_{cc}^{-1} \\ Z'_{dd} &= \tilde{Y}_{dd}^{-1} - \tilde{Y}_{dd}^{-1} C_{dr} \tilde{Z}_{rr}^{-1} C_{rd}^t \tilde{Y}_{dd}^{-1} \end{aligned} \quad \text{(A1.8)}$$

and

$$\tilde{Z}_{rr} = Z_{rr} + C_{rc}^t \tilde{Y}_{cc}^{-1} C_{cr} + C_{rd}^t \tilde{Y}_{dd}^{-1} C_{dr}, \quad \text{(A1.9)}$$

Z_{rr} is the local Z matrix formed by r removed brances, and C_{cr} and C_{dr} are the connection matrices local to the subnetworks c and d.

Substituting (A1.3) to (A1.9) in (A1.1) and (A1.2) the following equations can be obtained to compute the nodal voltages

$$\begin{aligned} V_a &= Z'_{aa} I_a - Z'_{ab} C_{bs} \tilde{Z}_{ss}^{-1} C_{sb}^t Z'_{ba} I_a \\ V_b &= Z'_{ba} I_a - Z'_{bb} C_{bs} \tilde{Z}_{sb}^{-1} C_{sb}^t Z'_{ba} I_a \\ V_c &= -Z'_{cc} C_{cs} \tilde{Z}_{ss}^{-1} C_{sb}^t Z'_{ba} I_a \\ V_d &= -Z'_{bc} C_{cs} \tilde{Z}_{ss}^{-1} C_{sb}^t Z'_{ba} I_a \end{aligned} \quad \text{(A1.10)}$$

The equations given in (A1.10) are used to develop a concurrent algorithm for implementation on a transputer ring.

REFERENCES

[1] S. Ramo, J. R. Whinnery, and T. Van Duzer, *Fields and Waves in Communication Electronics*. New York: Wiley, 1965.
[2] G. Kron, "Equivalent circuit of field equations of Maxwell-I," *Proc. IRE*, vol. 32, pp. 289–299, 1944.
[3] K. Spangenberg, G. Walters, and F. Schott, "Electrical network analyzers for the solution of electromagnetic field problems," *Proc. IRE*, vol. 37, pp. 724–729, 1949.
[4] V. F. Fusco and L. N. Merugu, "Concurrent algorithms for E.M. field mapping of passive microwave circuits," *IEE Colloquium on Field Analysis of Microwave Devices and Circuits, Digest 1991/015*, pp. 6.1–6.4, London, Jan. 1991.
[5] G. Kron, *Diakoptics-The Piecewise Solution of Large Scale Systems*, Macdonald, 1963.
[6] ——, "A method of solving very large physical systems in easy stages," *Proc. IRE*, pp. 680–686, Apr. 1954.
[7] G. Goubau, N. N. Puri, and F. K. Schwering, "Diakoptic theory for multi element antennas," *IEEE Trans. Antennas Propagat.*, vol. AP-30, no. 1, pp. 15–26, Jan. 1982.
[8] F. Schwering, N. N. Puri, and C. M. Butler, "Modified diakoptic theory of antennas," *IEEE Trans. Antennas Propagat.*, vol. AP-34, no. 11, pp. 1273–1281, Nov. 1986.
[9] C. M. Butler, "Diakoptic and the moment method," *1990 IEEE AP-S Int. Microwave Symp.*, 1990, pp. 72–75.
[10] G. E. Howard and Y. L. Chow, "Diakoptic theory for microstripline structures," *1990 IEEE AP-S Microwave Symp*, pp. 1079–1082.
[11] G. E. Howard and Y. L. Chow, "A high level compiler for the electromagnetic modelling of complex circuits by geometrical partitioning," *1991 IEEE MTT-S Int Microwave Symp Dig.*, pp. 1095–1098.
[12] C. R. Brewitt-Taylor and P. B. Johns, "On the construction and numerical solution of transmission-line and lumped network models of Maxwell's equations," *Int. J. Num. Meth. Eng.*, vol. 15, pp. 13–30, 1980.
[13] W. Geyi, "Numerical solution of transmission line problems by a network model decomposition method based on polygon discretization,"

IEEE Trans. Microwave Theory Tech., vol. 38, no. 8, pp. 1086–1091, Aug. 1990.
[14] A. Brameller, M. N. John, and M. R. Scott, *Practical Diakoptics for Electrical Networks*, Chapman and Hall, 1969.
[15] R. W. Hockney and C. R. Jesshope, *Parallel Computers 2 - Architecture, Programming and Algorithms*, Adam Hilger, 1988.
[16] G. Harp, Ed., *Transputer Applications*, Pitman, 1989.
[17] D. K. Tatalias, "Mapping Electromagnetic Field Computations to Parallel Processors," *IEEE Trans. Magn.*, vol. 25, no. 4, pp. 2901–2906, 1989.
[18] M. Swaminathan and T. K. Sarkar, "Parallel computation of electromagnetic scattering from arbitrary structures," *IEEE Trans. Magn.*, vol. 25, no. 4, pp. 2890–2891, 1989.
[19] R. H. Calalo, T. A. Cwik, W. A. Imbraile, N. Jacobi, P. C. Liewer, T. G. Lockhart, G. A. Lyzenga, and J. E. Patterson, "Hypercube parallel architectures applied to electromagnetic scattering analysis," *IEEE Trans. Magn.*, vol. 25, no. 4, pp. 2898–2900, July 1989.
[20] E. N. Opp, S. L. Geyer, R. Thomas, M. S. Willet, and K. Umashankar, "Numerical computation of electromagnetic scattering on the connection machine using method of moments," *IEEE Trans. Magn.*, vol. 25, no. 4, pp. 2907–2909, July 1989.
[21] D. B. Davidson, "A parallel processing tutorial," *IEEE Antennas and Propagation Society Magazine*, pp. 6–19, Apr. 1990.
[22] C. Hafner, "Parallel computation of electromagnetic fields on transputers," *IEEE Antennas and Propagation Society Newsletter*, pp. 6–12, Oct. 1989.
[23] V. F. Fusco, "Concurrent processing: The key to rapid probabilistic potential methods," *Int. J. Numerical Modelling: Electronic Networks, Devices and Fields*, vol. 3, pp. 1–9, 1990.
[24] L. N. Merugu, V. F. Fusco, and J. A. C. Stewart, "Network folding strategies for concurrent electromagnetic field mapping," *1991 IEEE MTT-S Int. Microwave Symp. Dig.*, Boston, June 10–14, vol. 1, pp. 349–352.
[25] V. F. Fusco and L. N. Merugu, "Network folding for large electrical network problems," in *Applications of Transputers 3*, vol. II, pp. 742–747, Glasgow: IOS Press, 1991.
[26] V. F. Fusco, L. N. Merugu, and D. S. McDowall, "Efficient diakoptics based algorithm for EM field mapping," *IEE Int. Conf. on Computation in Electromagnetics*, Conf. Pub. No. 305, pp. 51–54, London, Nov. 1991.
[27] W. K. Gwarek, "Analysis of an arbitrarily shaped planar circuit-A time domain approach," *IEEE Trans. Microwave Theory Tech.*, vol. MTT-33, no. 10, pp. 1067–1072, Oct. 1985.
[28] K. C. Gupta, "Multiport network approach for modelling and analysis of microstrip patch antennas and arrays," *IEE, in Handbook of Microstrip Antennas*, vol. 1, ch. 9, J. R. James and P. S. Hall, Eds., 1989.
[29] I. S. Duff, "The Impact of Parallelism on Numerical Methods," in *Major Advances in Parallel Processing*, Chris Jesshope, Ed., 1987, pp. 255–263.
[30] *Parallel Fortran User Guide*, 3L Ltd., Livingstone, Scotland, 1988.
[31] T. Okoshi, *Planar Circuits for Microwaves and Light Waves*. New York: Springer-Verlag, 1985.
[32] I. Wolff, G. Kompa, and R. Mehran, "Calculation method for microstrip discontinuities and T Junctions," *Electron. Lett.*, vol. 8, no. 7, pp. 177–179, 1972.
[33] G. Kompa and G. Mehran, "Planar waveguide model for calculating microstrip components," *Electron. Lett.*, vol. 11, no. 9, pp. 459–460, 1975.
[34] L. N. Merugu, V. F. Fusco, and J. A. C. Stewart, "A phase quadrature square patch microwave coupler," *Microwave and Optical Tech. Lett.*, vol. 2, no. 12, pp. 424–427, Dec. 1989.
[35] K. A. Gallivan, *Parallel Algorithms for Matrix Computations*, Siam, 1991.

L. N. Merugu (M'92) graduated with the degree of M.Tech. from the Indian Institute of Technology Kharagpur in 1980 and with the degree of Ph.D. from the Queen's University of Belfast in 1991.

Currently, he is employed as a research scientist at the Defense Electronics Research Laboratory, Hyderabad, India. Research interests include antenna design and the numerical modelling of passive electromagnetic circuits, in which areas he has published a number of papers.

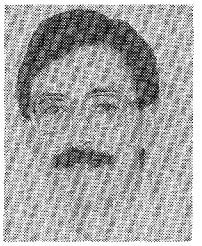

Vincent F. Fusco was educated at the Queen's University of Belfast where he obtained the degree of Ph.D.

He has worked as a research engineer on short range radar and radio telemetry systems. Currently he is a reader in Microwave Communications in the School of Electrical Engineering and Computer Science, The Queen's University of Belfast. His current research interests include nonlinear microwave circuit simulation and concurrent programming techniques for electromagnetic field problems. He has acted as consultant to a number of major companies and has published numerous research papers in these areas. He is author of the book Microwave Circuits, Analysis and Computer Aided Design, Prentice Hall, 1987.

Dr. Fusco is a Chartered Electrical Engineer and a Member of the Institute of Electrical Engineers.